PERSPECTIVE

Ultrafast dynamics of electron-phonon coupling in a metal

To cite this article: Choongyu Hwang *et al* 2019 *EPL* **126** 57001

A Letters Journal Exploring the Frontiers of Physics

June 2019

EPL, **126** (2019) 57001 www.epljournal.org
doi: 10.1209/0295-5075/126/57001

Perspective

Ultrafast dynamics of electron-phonon coupling in a metal

Choongyu Hwang[1,2], Wentao Zhang[2,3], Koshi Kurashima[4], Robert Kaindl[2], Tadashi Adachi[4,5], Yoji Koike[4] and Alessandra Lanzara[2,6]

[1] *Department of Physics, Pusan National University - Busan 46241, South Korea*
[2] *Materials Sciences Division, Lawrence Berkeley National Laboratory - Berkeley, CA 94720, USA*
[3] *School of Physics and Astronomy, Shanghai Jiao Tong University - Shanghai 200240, China*
[4] *Department of Applied Physics, Tohoku University - Sendai 980-8579, Japan*
[5] *Department of Engineering and Applied Sciences, Sophia University - Tokyo 102-8554, Japan*
[6] *Department of Physics, University of California - Berkeley, CA 94720, USA*

received 13 April 2019; accepted in final form 17 June 2019
published online 27 June 2019

PACS 78.47.J- – Ultrafast spectroscopy (<1 psec)
PACS 74.25.Jb – Electronic structure (photoemission, etc.)
PACS 71.38.-k – Polarons and electron-phonon interactions

Abstract – In the past decade, the advent of time-resolved spectroscopic tools has provided a new ground to explore fundamental interactions in solids and to disentangle degrees of freedom whose coupling leads to broad structures in the frequency domain. Time- and angle-resolved photoemission spectroscopy (tr-ARPES) has been utilized to directly study the relaxation dynamics of a metal in the presence of electron-phonon coupling. The effect of photo-excitations on the real and imaginary part of the self-energy as well as the time scale associated with different recombination processes are discussed. In contrast with a theoretical model, the phonon energy does not set a clear scale governing quasiparticle dynamics, which is also different from the results observed in a superconducting material. These results point to the need for a more complete theoretical framework to understand electron-phonon interaction in a photo-excited state.

Introduction. – In the past decade, the advancement of laser technology has allowed the extension of spectroscopic tools into the time domain. This has opened a new range of opportunities, especially when it comes to the study of complex materials where more than one interaction is at play and degrees of freedom are often strongly intertwined. This has lead to an unprecedented access to fundamental elementary interactions in materials at their natural time scales. Among them major emphasis has been dedicated both theoretically and experimentally to the study of electron-phonon coupling that drives new ground states such as superconductivity, Peierls transition etc.

Angle-resolved photoemission spectroscopy (ARPES) is the ideal tool to study the electron-phonon interaction, as it can directly probe the quasiparticles dispersion, Fermi velocity, and self-energy renormalization. Moreover, its ability to resolve such interactions in a momentum space provides unique information on the anisotropy of such interaction. Given the recent extension of ARPES to the time domain, indeed, electron-phonon coupling can be measured and disentangled from other energy/time scales by directly measuring the relaxation channels of hot electronic distribution in a transient state [1–3].

The electron-phonon coupling is also a limiting factor of intrinsic mobility of charge carriers via ultrafast energy dissipation [4–6]. Especially in metals, the electron-phonon coupling leads to a faster relaxation of excited electrons through emitting phonons, when the energy of the excited electrons is higher than the phonon energy. This relatively slower and faster dynamics across the phonon energy generates an energy cut-off in the transient spectra, also known as cut-off energy, and observed in high-temperature superconductors [7,8]. However, most of the experimental works so far have focused on the relaxation dynamics of superconductors. In order to have a full understanding and be able to disentangle other interactions, we first need to learn how electron-phonon interaction, in general, responds to photo-excitations.

Here, a metallic system has been examined using time-resolved ARPES (tr-ARPES). Due to an optical excitation, electrons are injected in the unoccupied states,

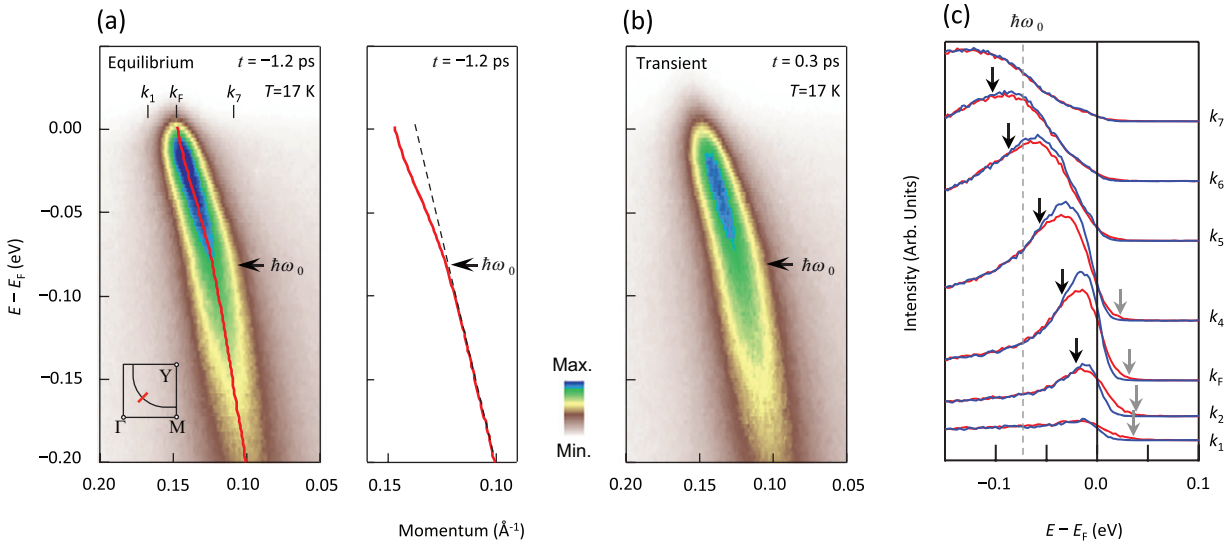

Fig. 1: (a), (b): equilibrium (a) and transient (b) ARPES intensity maps taken at $t = -1.2$ ps and $t = 0.3$ ps, respectively. Both energy maps were taken along the diagonal direction of the Brillouin zone denoted by the red line in the inset of panel (a). Pump fluence is $30\,\mu$J/cm^2. The red curve is the Lorentzian fit to momentum distribution curves taken from the ARPES intensity map measured at $t = -1.2$ ps and the black dashed line is a guide to the eyes. The phonon energy is denoted by $\hbar\omega_0$. (c) Energy distribution curves for equilibrium (blue) and transient (red) maps taken at different momentum values from k_1 to k_7 denoted in panel (a).

transferring spectral weight toward lower-energy states via emitting phonons. In contrast with the predicted behavior [9,10] and experimental observation in cuprates superconductors [3,7], we find that, in the metallic state, the relaxation process gradually increases as the excited carrier density increases (*e.g.*, by increasing the pump fluence), without a clear energy cut-off that distinguishes slow *vs.* fast dynamics across the phonon energy. These results point to the need for a more complete theoretical framework to understand the electron-phonon interaction in a photo-excited state as well as more detailed work to understand the role that such cut-off energy can play for superconductivity [10].

Methods. – The time-resolved ARPES measurements were performed at 17 K on heavily overdoped $Bi_{1.76}Pb_{0.35}Sr_{1.89}CuO_{6+\delta}$, which is known to be in a metallic phase. The laser system is a cavity-dumped, mode-locked Ti:sapphire oscillator (Coherent Mira) generating ≈150 fs pulses at 840 nm at a repetition rate of 54.3/n MHz ($n = 1, 2, 3, \ldots$), whose details are described elsewhere [11]. A transient state is created with an infrared laser pump pulse with an energy of 1.48 eV and measured via photoemission process as a function of the delay time with a resolution of 300 fs using an ultraviolet probe pulse with an energy of 5.9 eV. The energy and momentum resolutions are 22 meV and 0.003 Å^{-1}, respectively. The pump fluence is varied from 4 to 24 μJ/cm^2.

Results and discussion. – Figures 1(a) and (b) show equilibrium and transient ARPES intensity maps at $t = -1.2$ ps and $t = 0.3$ ps, respectively. Here $t = 0$ represents the time when pump and probe pulses are applied to the sample simultaneously. Negative time refers to equilibrium spectra, *e.g.*, spectra taken before the arrival of the pump pulse, while positive time refers to transient spectra, *e.g.*, after the sample has been excited by the pump pulse.

The data were taken along the Brillouin zone diagonal denoted by the red line in the inset of fig. 1(a), using a pump fluence of 24 μJ/cm^2. The sample temperature in the equilibrium state was $T = 17$ K, measured using a diode thermally connected to the sample. In both maps, one can identify a characteristic energy $\hbar\omega_0 \sim 70$ meV (denoted by an arrow) that separates a well-defined and poorly defined dispersive features above and below it, respectively, with different slopes (the black curve is a Lorentzian fit to momentum distribution curves and the black dashed line is an arbitrary straight line for the guide to the eyes). The change in the slope of the energy spectra, so-called a kink, is a universal feature of cuprates due to electron-phonon coupling, especially in the absence of competing phases against superconductivity in the heavily overdoped regime [12]. The main effect of the pump pulse is to change the spectral intensity. Figure 1(c) shows energy distribution curves at momentum positions from k_1 to k_7, denoted in fig. 1(a), for equilibrium (blue curve) and transient (red curve) maps. The spectra are normalized by the intensity at higher energy ($-0.20\,\text{eV} \leq E - E_\text{F} \leq -0.18\,\text{eV}$) for comparison.

This change in the transient map is clearly evidenced when its photoelectron intensity is subtracted by that of the equilibrium map as shown in fig. 2(a): loss (gain) in

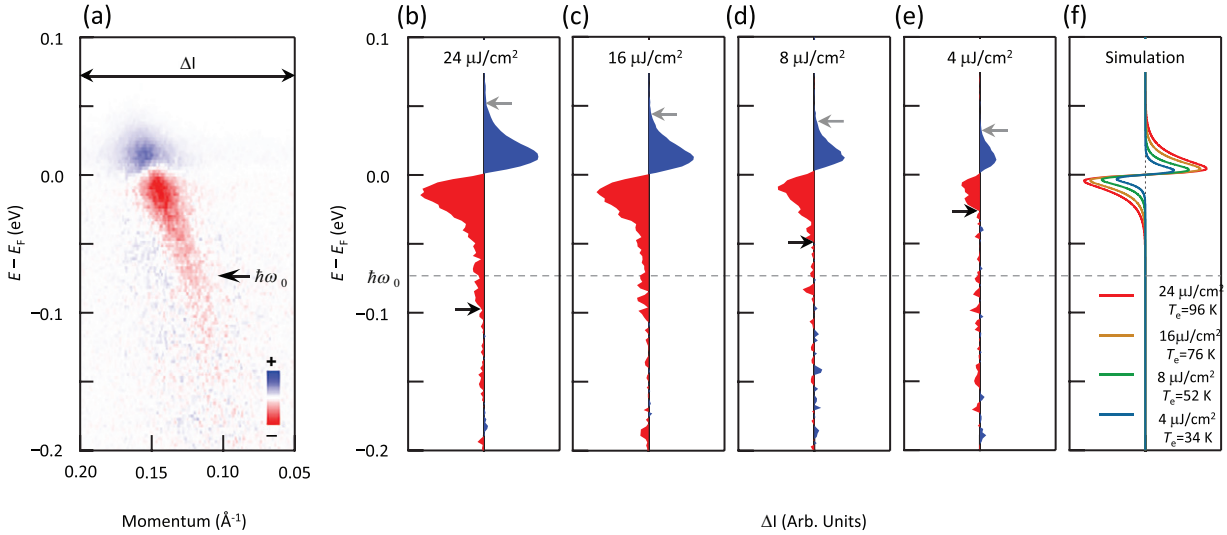

Fig. 2: (a) Intensity difference map between before and after applying the laser pump pulse shown in figs. 1(a) and (b), respectively. (b)–(e) Momentum-integrated spectra (ΔI), from 0.05 Å^{-1} to 0.20 Å^{-1} in panel (a), for four different pump fluences. (f) Simulation of ΔI assuming the transient heating effect by the pump pulse. Electronic temperature T_e at $t = 0.3$ ps is 96, 76, 52, and 34 K for a pump fluence of 24, 16, 8, and 4 μJ/cm^2, respectively.

spectral intensity is denoted by red (blue) color. Figures 2(b)–(e) show the integrated intensity (ΔI) over a momentum range from 0.05 to 0.20 Å^{-1}. At 24 μJ/cm^2, most of the intensity change is observed near E_F as shown in fig. 2(b). However, the intensity change persists beyond $\hbar\omega_0$ down to $E - E_F \sim -100$ meV (denoted by a black arrow). Upon decreasing the pump fluence, the cut-off energy is also decreasing to ~ -50 meV at 8 μJ/cm^2 as shown in fig. 2(d) and ~ -30 meV at 4 μJ/cm^2 as shown in fig. 2(e). The overall decrease of ΔI is due to the decreasing pump fluence that excites less electrons to a transient state. Additionally, the cut-off energy above E_F is far below $\hbar\omega_0$ at 24 μJ/cm^2 as denoted by a gray arrow in fig. 2(b) and approaches toward E_F with decreasing pump fluence. Such a spectral change cannot be explained by thermal smearing of the Fermi edge due to the transient heating effect by the pump pulse, because the observed cut-off energy is higher than the cut-off energy expected from the electronic temperature (T_e) increased by the pump pulse, *e.g.*, fig. 2(f) shows the difference of Fermi-Dirac distribution at T_e from that at the equilibrium temperature, 17 K. These observations are in contrast with a proposed model where the intensity cut-off originates from the electron-boson coupling [9].

Such coupling provides a fast decay channel for electron (hole) excitations above (below) the boson energy. High-energy excitations can decay by emitting (absorbing) a boson. Boson-mediated decay is predicted to reduce the lifetime of quasiparticles to tens of femtoseconds. Along this line, the efficacy of this additional bypass is determined by the electron-boson coupling strength, which can be measured by the kink strength. However, the kink strength of $Bi_{1.76}Pb_{0.35}Sr_{1.89}CuO_{6+\delta}$ is roughly similar across different doping and temperature. This apparent inconsistency can be explained by the difference between the single-particle lifetime (which can be extracted from the self-energies) and the population lifetime (the quantity ARPES is measuring) [13]. The difference exists when an energy conserving decay channel, for instance, Coulomb and elastic impurity scattering, is present [13,14]. When a single particle decays through such a channel where energy is retained in the electronic system, another excitation is created. As the process cascades, the population takes much longer to vanish after than the single-particle time scale.

This intensity change is accompanied by an intriguing time-dependence of the electron self-energy as shown in fig. 3. Within the Debye model, both real and imaginary parts of electron self-energies are affected by the electron-phonon coupling [15–17]. In other words, electrons acquire renormalized mass as well as enhanced scattering through the coupling to a phonon [16]. Indeed, the real part of the electron self-energy, ReΣ, shown in fig. 3(a), obtained by subtracting a bare or unrenormalized band (assumed to be a linear band) from the measured or renormalized energy spectrum shown in figs. 1(a) and (b), exhibits a peak-like shape around $\hbar\omega_0$ due to the electron-phonon coupling, consistent with previous reports on cuprates [12,16,17]. Upon applying the laser pump pulse at 24 μJ/cm^2, ReΣ decreases from the blue filled circle at $t = -1.2$ ps to the red filled circle at $t = 0.3$ ps, when the difference, ΔReΣ, is denoted by the gray shaded area. ReΣ is recovered back to the almost original shape after longer delay time at $t = 10.2$ ps, denoted by blue empty circles. Hence, the electron-phonon coupling is suppressed upon applying a laser pump pulse by ~14%, determined by the change of slope of ReΣ near E_F, with a line fit to the data from -50 meV to -20 meV shown as black lines, and

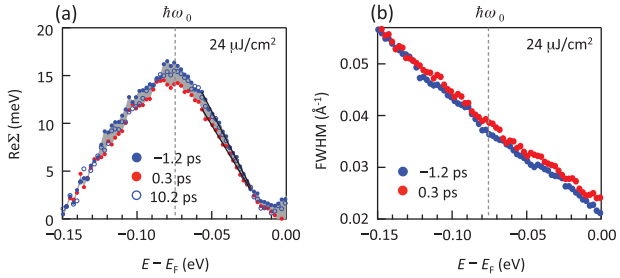

Fig. 3: (a) Real part of the electron self-energy (ReΣ) before ($t = -1.2$ ps) and after ($t = 0.3$ ps and 10.2 ps) applying the laser pump pulse. (b) Full width at half maximum (FWHM) of the energy spectra before ($t = -1.2$ ps) and after ($t = 0.3$ ps and 10.2 ps) applying the laser pump pulse with three difference fluences.

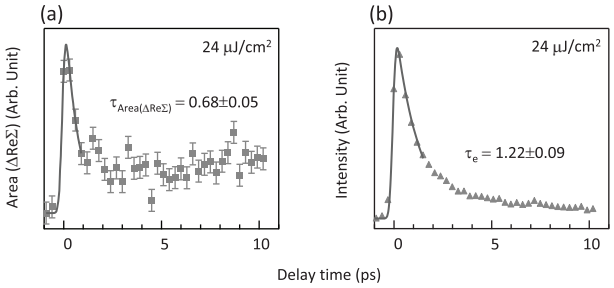

Fig. 4: (a) The area of the difference in the electron self-energy as a function of delay time. The solid curve is an exponential least-square fit to extract the time constant of 0.68 ± 0.05 ps. (b) Averaged spectral intensity above E_F as a function of the delay time. The solid curve is an exponential least-square fit to extract the time constant of 1.22 ± 0.09 ps.

recovered afterward. A similar self-energy change is observed when the pump pulse is incident on a superconducting cuprate [3]. However, a critical difference is that for a non-superconducting cuprate, the overall self-energy is depressed by the pump pulse even below the phonon energy $\hbar\omega_0$. On the other hand, for a superconducting cuprate, the self-energy change is prominent mostly for a self-energy peak at $\hbar\omega_0$, whereas for the others the self-energy change is barely observed.

Figure 3(b) shows the full width at half maximum (FWHM) of the momentum distribution curves taken as a function of $E - E_F$ for the measured energy spectra shown in figs. 1(a) and (b). FWHM is considered to be linearly proportional to the imaginary part of the electron self-energy (ImΣ) by FWHM $= 2|\mathrm{Im}\Sigma/v|$, where v is the bare velocity. Upon applying the laser pump pulse at 24 μJ/cm^2, FWHM at E_F is enhanced by ∼14%, indicating the suppression of the electron-phonon coupling. With decreasing $E - E_F$, however, the difference gradually decreases until it becomes negligible at $E - E_F \sim 0.12$ eV. Consistently with the ReΣ, while the biggest changes occur at lower binding energy, the pump-induced changes are also reflected above the phonon energy. The change in ReΣ and FWHM indicates that electronic excitation suppresses the strength of electron-phonon coupling in a transient state with respect to an equilibrium state and that the suppression is recovered as a function of time. This hinders to extract the strength of electron-phonon coupling in an equilibrium state from the dynamics of electrons in a transient state, in contrast with the claim of the previous theoretical work on a non-superconducting metal [9].

To further understand the time-dependent electron-phonon coupling, the dynamics of ΔReΣ has been studied as a function of delay time and compared to the quasiparticle dynamics as extracted from the integrated intensity above E_F [7]. The area of ΔReΣ for an energy range of $-0.15\,\mathrm{eV} \le E - E_F \le -0.02\,\mathrm{eV}$ shows an initial sharp increase near $t = 0$ with a pump fluence of 24 μJ/cm^2 that is relaxed with increasing delay time. The solid line in fig. 4(a) is an exponential least-square fit to Area (ΔReΣ) that gives a time constant, $\tau_{\mathrm{Area}}(\Delta\mathrm{Re}\Sigma)$, of 0.68 ± 0.05 ps. Interestingly, the time scale, associated with the kink, is by a factor of two smaller than the relaxation time of quasiparticles: τ_e of 1.22 ± 0.09 ps as shown in fig. 4(b). A similar difference between the two time scales has been also observed for cuprates superconductors [3]. However, $\tau_{\mathrm{Area}}(\Delta\mathrm{Re}\Sigma)$ is almost 5 times faster than the one in a superconducting cuprate, *e.g.*, 3.12 ps for $Bi_2Sr_2CaCu_2O_{8+\delta}$ [3] *vs.* 0.68 ps for the non-superconducting cuprate observed in fig. 4(a), at the same pump fluence. In other words, the suppressed coupling between electrons and phonons is recombined even faster in a non-superconducting (and metallic) cuprate than for a superconducting cuprate.

Indeed in a metallic system, the electron population resembles a thermal population that is the case of a non-superconducting cuprate. In contrast, when a gap opens in a superconducting cuprate, electron relaxation dynamics become coupled to the dynamics of the electron population and phase restriction processes kick in, leading to coexisting femtosecond and picosecond dynamics [18]. Clearly these results suggest that there are several mechanism at play that could provide new insights on the nature of the superconductivity and ask for more detailed theoretical works.

Summary. – We have shown that, in a non-superconducting cuprate, *i.e.*, a metallic system, the electron-phonon coupling is perturbed by a femtosecond laser pump pulse in contrast with the theoretical prediction and that the perturbation is relaxed in a faster time scale compared to that in a superconducting cuprate. In addition, the suppressed coupling between electrons and phonons is recombined even faster in a non-superconducting cuprate than in a superconducting cuprate, suggesting the possibility that several mechanism may play an important role in electronic dynamics in the high-temperature superconductivity. Our results not only provide the time scale of the coupling formation between

electrons and phonons in a non-superconducting system, but also invite a more complete theoretical framework to understand electron-phonon interaction in a photo-excited state.

* * *

This work was primarily supported by Berkeley Lab's program on Ultrafast Materials Sciences, funded by the U.S. Department of Energy, Office of Science, Office of Basic Energy Sciences, Materials Sciences and Engineering Division, under contract DE-AC02-05CH11231. CH also acknowledges support from the National Research Foundation of Korea (NRF) grant funded by the Korea government (MSIT) (No. 2017K1A3A7A09016384 and No. 2018R1A2B6004538).

REFERENCES

[1] Siegel D. A., Hwang C., Fedorov A. V. and Lanzara A., *New J. Phys.*, **14** (2012) 095006.
[2] Calandra M. and Mauri F., *Phys. Rev. B*, **76** (2007) 205411.
[3] Zhang W., Hwang C., Smallwood C. L., Miller T. L., Affeldt G., Kurashima K., Jozwiak C., Eisaki H., Adachi T., Koike Y., Lee D.-H. and Lanzara A., *Nat. Commun.*, **5** (2014) 4959.
[4] Millis A. J., Littlewood P. B. and Shraiman B. I., *Phys. Rev. Lett.*, **74** (1995) 5144.
[5] Allen P. B., *Phys. Rev. B*, **36** (1987) 2920.
[6] Chen J.-H., Jang C., Xiao S., Ishigami M. and Fuhrer M. S., *Nat. Nanotechnol.*, **3** (2008) 206.
[7] Graf J., Jozwiak C., Smallwood C. L., Eisaki H., Kaindl R. A., Lee D.-H. and Lanzara A., *Nat. Phys.*, **7** (2011) 805.
[8] Smallwood C. L., Hinton J. P., Jozwiak C., Zhang W., Koralek J. D., Eisaki H., Lee D.-H., Orenstain J. and Lanzara A., *Science*, **336** (2012) 1137.
[9] Sentef M., Kemper A., Alexander F., Moritz B., Freericks J. K., Shen Z.-X. and Devereaux T. P., *Phys. Rev. X*, **3** (2013) 041033.
[10] Miller T. L., Zhang W., Ma J., Eisaki H., Moore J. E. and Lanzara A., *Phys. Rev. B*, **97** (2018) 134517.
[11] Graf J., Hellmann S., Jozwiak C., Smallwood C. L., Hussain Z., Kaindl R. A., Kipp L., Rossnagel K. and Lanzara A., *J. Appl. Phys.*, **107** (2010) 014912.
[12] Lanzara A., Bogdanov P. V., Zhou X. J., Kellar S. A., Feng D. L., Lu E. D., Yoshida T., Eisaki H., Fujimori A., Kishio K., Shimoyama J.-I., Noda T., Uchida S., Hussain Z. and Shen Z.-X., *Nature*, **412** (2001) 510.
[13] Yang S.-L., Sobota J. A., Leuenberger D., He Y., Hashimoto M., Lu D. H., Eisaki H., Kirchmann P. S. and Shen Z.-X., *Phys. Rev. Lett.*, **114** (2015) 247001.
[14] Rameau J. D., Freutel S., Kemper A. F., Sentef M. A., Freericks J. K., Avigo I., Ligges M., Rettig L., Yoshida Y., Eisaki H., Schneeloch J., Zhong R. D., Xu Z. J., Gu G. D., Johnson P. D. and Bovensiepen U., *Nat. Commun.*, **7** (2016) 13761.
[15] Hengsberger M., *Phys. Rev. B*, **60** (1999) 10796.
[16] Verga S., Knigavko A. and Marsiglio F., *Phys. Rev. B*, **67** (2003) 054503.
[17] Reinert F. and Hüfner S., *New J. Phys.*, **7** (2005) 97.
[18] Smallwood C. L., Miller T. L., Zhang W., Kaindl R. L. and Lanzara A., *Phys. Rev. B*, **93** (2016) 235107.